Radiation Effects & Defects in Solids
Vol. 164, No. 4, April 2009, 266–275

Taylor & Francis
Taylor & Francis Group

Kinetic studies for the non-isothermal decomposition of un-irradiated and γ-irradiated ruthenium(III) acetylacetonate

R.M. Mahfouz[a]*, Sh.A. Al-Ahmari[a], I.Kh. Warad[a], S.I. Al-Resayes[a], M.R.H. Siddiqui[a], K.R. Raslan[b] and A.M. Al-Otaibi[a]

[a]*Department of Chemistry, College of Science, King Saud University, PO Box 2455, Riyadh-11451, Saudi Arabia;* [b]*Natural Science (Mathematics), Community College of Science, King Saud University, Riyadh, Saudi Arabia*

(*Received 21 March 2007; final version received 20 April 2007*)

Kinetic studies for the non-isothermal decomposition of un-irradiated and γ-irradiated ruthenium(III) acetylacetonate in air were carried out. The results show that the decomposition proceeds in one major step in the temperature range of 150–250 °C with the formation of RuO_2 as a final solid residue for un-irradiated $Ru(acac)_3$. For γ-irradiated $Ru(acac)_3$ with 10^2 KGy total γ-ray dose, the decomposition goes eventually to completion with almost 100% decomposition and proceeds in one major step, which contains four overlapping decomposition stages in the temperature range of 200–320 °C. The kinetics is shown to be non-isothermal, using both model-fitting and model-free approaches. Infrared (IR) spectroscopy and X-ray powder diffraction techniques were employed to follow the chemical composition of the solid residue obtained at different temperatures.

Keywords: $Ru(acac)_3$; non-isothermal decomposition; γ-irradiation; nanoparticles

1. Introduction

Thermal decomposition of solids is an important field of solid-state chemistry with wide technical applications. Many recent studies on the thermal decomposition of inorganic solids have included measurements on samples that were exposed to radiation prior to heating, with the view to investigate the effects of ionizing radiation on the thermal decomposition behaviour. For instance, radiation can modify one or more properties of the material in an important way by creating point defects or by increasing the number of nucleation forming sites. The kinetics of the thermal decomposition of inorganic materials could be affected markedly by prior exposure to ionizing radiation, *i.e.*, by the shortening of the induction period followed by an overall decrease in time needed to complete the reaction.

*Corresponding author. Email: rmhfouz@ksu.edu.sa

ISSN 1042-0150 print/ISSN 1029-4953 online

DOI: 10.1080/10420150701414272
http://www.informaworld.com

Ruthenium(III) acetylacetonate, $Ru(acac)_3$, is considered as a promising precursor for the synthesis of heterogeneous ruthenium catalysts that are active in hydrogenolysis, isomerization and hydrogenation of hydrocarbons (*1–3*). $Ru(acac)_3$ is a suitable metallic organic compound for the preparation of RuO_2, which plays an important role in many applications in catalysis, electrochemistry and electronic technology (*4–5*). Thermal decomposition of un-irradiated $Ru(acac)_3$ in air has been studied by Music et al. (*6*). Thermolysis of $Ru(acac)_3$ supported on silica and alumina has been investigated by Yuri. V et al. (*7*). The results of these studies indicated that RuO_2 is the solid product of the decomposition without giving any details for the kinetics of the thermal decomposition of $Ru(acac)_3$. No studies are reported for the mechanism controlling the decomposition or the kinetic and thermodynamic parameters of the decomposition.

In the present work, the thermal decomposition behaviour of un-irradiated and γ-irradiated $Ru(acac)_3$ was investigated in air in order to shed more light on the kinetics of thermal decomposition of $Ru(acac)_3$ and the role of ionizing radiation on the thermal behaviour of $Ru(acac)_3$.

2. Experimental

Ruthenium acetylacetonate was obtained commercially from Aldrich Ltd. and used without further purification. Samples were dried in a disccator before analysis. For the thermal experiments, a thermogravimetric analyser was used (TGA-7, Perkin–Elmer). The amount of the sample was kept at 10 ± 0.1 mg. Under dynamic (non-isothermal) conditions four linear heating rates (5, 10, 15, 20 °C/min) were applied.

For irradiation, samples were encapsulated under vacuum in glass vials and exposed to successively increasing doses of radiation at constant intensity using a Co-60 γ-ray cell 220 (Nordion INT – INC, Ontario, Canada) at a dose rate of 10^4 Gy/h. The source was calibrated against a Fricke ferrous sulphate dosimeter and the dose rate in the irradiated samples was calculated by applying appropriate corrections on the basis of both the photon mass attenuation and energy absorption coefficient for the sample and dosimeter solutions (*8*).

The fraction decomposed or the extent of conversion of α was calculated as

$$\alpha = \frac{M_o - M}{M - M_f},$$

where M_o, M, M_f are the initial, actual and final sample masses, respectively.

The infrared (IR) spectra were recorded as KBr pellets using a Perkin–Elmer 1000 FT-IR spectrophotometer. XRD measurements were carried out on a Siemens D5000 X-ray diffractometer using a nickel filter (Cu Kα, $\lambda = 1.5418$ Å).

3. Theory

A single-step process for solid state decomposition has the following kinetic equation

$$\frac{d\alpha}{dt} = K(T) f(\alpha), \tag{1}$$

where α is the extent of conversion, $K(T)$ is a temperature dependent reaction rate constant, and $f(\alpha)$ is a kinetic dependent model function.

Table 1. Set of reaction models applied to describe thermal decomposition in solids.

Reaction model		$f(\alpha)$	$g(\alpha)$	
1	Power law	$4\alpha^{3/4}$	$\alpha^{1/4}$	P_1
2	Power law	$3\alpha^{2/3}$	$\alpha^{1/3}$	P_2
3	Power law	$2\alpha^{1/2}$	$\alpha^{1/2}$	P_3
4	Power law	$2/3\alpha^{-1/2}$	$\alpha^{3/2}$	P_4
5	One-dimensional diffusion	$(1/2)\alpha^{-1}$	α^2	D_1
6	Mampel (first-order)	$1-\alpha$	$-\ln(1-\alpha)$	F_1
7	Avrmi-Erpfeev	$4(1-\alpha)[-\ln(1-\alpha)]^{3/4}$	$[-\ln(1-\alpha)]^{1/4}$	
8	Avrmi-Erpfeev	$3(1-\alpha)[-\ln(1-\alpha)]^{2/3}$	$[-\ln(1-\alpha)]^{1/3}$	
9	Avrmi-Erpfee	$2(1-\alpha)[-\ln(1-\alpha)]^{1/2}$	$[-\ln(1-\alpha)]^{1/2}$	
10	Three-dimensional diffusion	$2(1-\alpha)^{2/3}(1-(1-\alpha)^{1/3})^{-1}$	$[1-(1-\alpha)^{1/3}]^2$	D_3
11	Contracting sphere	$3(1-\alpha)^{2/3}$	$1-(1-\alpha)^{1/3}$	R_3
12	Contracting cylinder	$2(1-\alpha)^{1/2}$	$1-(1-\alpha)^{1/2}$	R_2
13	Second-order	$(1-\alpha)^2$	$(1-\alpha)^{-1}-1$	

The Arrhenius equation generally expresses the explicit temperature dependency of the rate constant as

$$\frac{d\alpha}{dt} = A\exp\left(\frac{-E_a}{RT}\right) f(\alpha). \tag{2}$$

The A, E, and $f(\alpha)$ are called the 'kinetic triplet' that can characterize a unique decomposition reaction. Some of the reaction models for solid state reactions are listed in Table 1. Under non-isothermal conditions in which a sample is heated at a constant rate, the explicit time dependence in Equation (1) is eliminated through the trivial transformation

$$\frac{d\alpha}{dT} = \frac{A}{\beta}\exp\left(\frac{-E_\alpha}{RT}\right) f(\alpha), \tag{3}$$

where $\beta = dT/dt$ is the heating rate.

3.1. *Model-fitting approach (Coats and Redfern method)*

Upon integration, Equation (3) gives

$$\begin{aligned} g(\alpha) = \int_0^\alpha \frac{d\alpha}{f(\alpha)} &= \frac{A}{\beta}\int_{T_0}^{T_\alpha} \exp\left(-\frac{E_a}{RT}\right) dT \\ &\approx \frac{A}{\beta}\int_0^{T_\alpha} \exp\left(-\frac{E_a}{RT}\right) dT = \frac{AE_a}{R\beta}\int_0^{T_\alpha} \frac{\exp(-x)}{x^2} dx \\ &= \frac{AE_a}{R\beta} P(x) \equiv \frac{A}{\beta} I(E_a, T), \end{aligned} \tag{4}$$

where $P(x)$ is the exponential integral for $x = E_a/RT$. The temperature integral $I(E_a, T)$ has no analytical solution but many approximations. One such approximation gives rise to the Coats–Redfern equation, (*9*):

$$\ln\left[\frac{g_j(\alpha)}{T^2}\right] = \ln\left(\frac{A_j R}{\beta E_j}\left[1-\left(\frac{2RT^*}{Ea_j}\right)\right]\right) - \frac{Ea_J}{RT}, \tag{5}$$

where T^* is the mean experimental temperature. Plotting the left-hand side, which includes the model $g(\alpha)$ of Equation (5) *vs.* $1/T$ gives E_a and $\ln A$ from the slope and intercept, respectively.

The goodness of fit is customarily estimated by a coefficient of linear correction r_j. A single pair of E_a and ln A is then commonly chosen as the one corresponding to a reaction model that gives rise to the maximum absolute value of the correlation coefficient [$r_{\max}$].

3.2. *Model-free approach (Vyazovkin (Vyz) method)*

A nonlinear iso-conversional method has been developed by Vyazovkin that avoids inaccuracies associated with analytical approximations of the temperature integral (*10*). For a set of n experiments carried out at different heating rates, the activation energy can be determined at any particular value of α by finding the value of E_a for which the objective function Ω is minimized, where

$$\Omega = \sum_{i=1}^{n} \sum_{j \neq i} \frac{I(E_\alpha, T_{\alpha,j})\beta j}{I(E_\alpha, T_{\alpha,i})\beta i} \tag{6a}$$

and

$$I(E_\alpha, T_{\alpha,i}) = \int_0^{T_{\alpha,i}} \exp\left(-\frac{E_{a,\alpha}}{RT}\right) \mathrm{d}T. \tag{6b}$$

The temperature integral can be evaluated by approximation of Cai et al. (*11*), where

$$\int_0^T \exp\left(-\frac{E_\alpha}{RT_{\alpha i}}\right) \mathrm{d}T = \frac{RT_{\alpha,i}^2}{E_\alpha} \left[\frac{(E_{a,\alpha}/RT_{\alpha i}) + 0.66691}{(E_{a,\alpha}/RT_{\alpha i}) + 2.64943}\right] \exp\left(\frac{-E_{a,\alpha}}{RT_{\alpha,i}}\right) \tag{7}$$

and by numerical integration.

Vyazovkin modified this method to account for variable heating rates and systematic errors in the activation energy in an advanced iso-conversional method based on the following Equation

$$\Omega = \sum_{i=1}^{n} \sum_{j \neq i}^{n} \frac{J(E_{a,\alpha}, T_i(t_\alpha))}{J(E_{a,\alpha}, T_J(t_\alpha))}, \tag{8}$$

where

$$J(E_a, T(t)) = \int_{t\alpha - \Delta\alpha}^{t\alpha} \mathrm{e}^{-Ea,\alpha/RT(t)} \, \mathrm{d}t, \tag{9}$$

for a linear heating function, $T(t) = T_0 + B(t)$ and $\Delta\alpha = (1/m)$ with m being the number of α segments chosen for integration (18 in our work). The integral ($J(E_a, T(t))$) was solved by numerical integration. The activation energy (E_a) is the value that minimizes Ω in Equation (8). All objective function minimizations were performed using the numerical methods in Mathematica. All kinds of integrations were solved using numerical methods with high accuracy.

4. Results

Figure 1 shows typical TG and DTA curves of un-irradiated $Ru(acac)_3$ in static air. The TG curve shows that the decomposition of $Ru(acac)_3$ proceeds in one major step in the temperature range of 150–250 °C with formation of RuO_2 as solid residue according to the following Equation.

$$Ru(acac)_3 \longrightarrow RuO_2 + \text{Volaties} \tag{10}$$

The acetylactonate ligand was found as the major gaseous product below 300 °C. At a temperature higher than 400 °C the gaseous acetylacetonate ligand decomposes mainly to CO, CO_2 and H_2O.

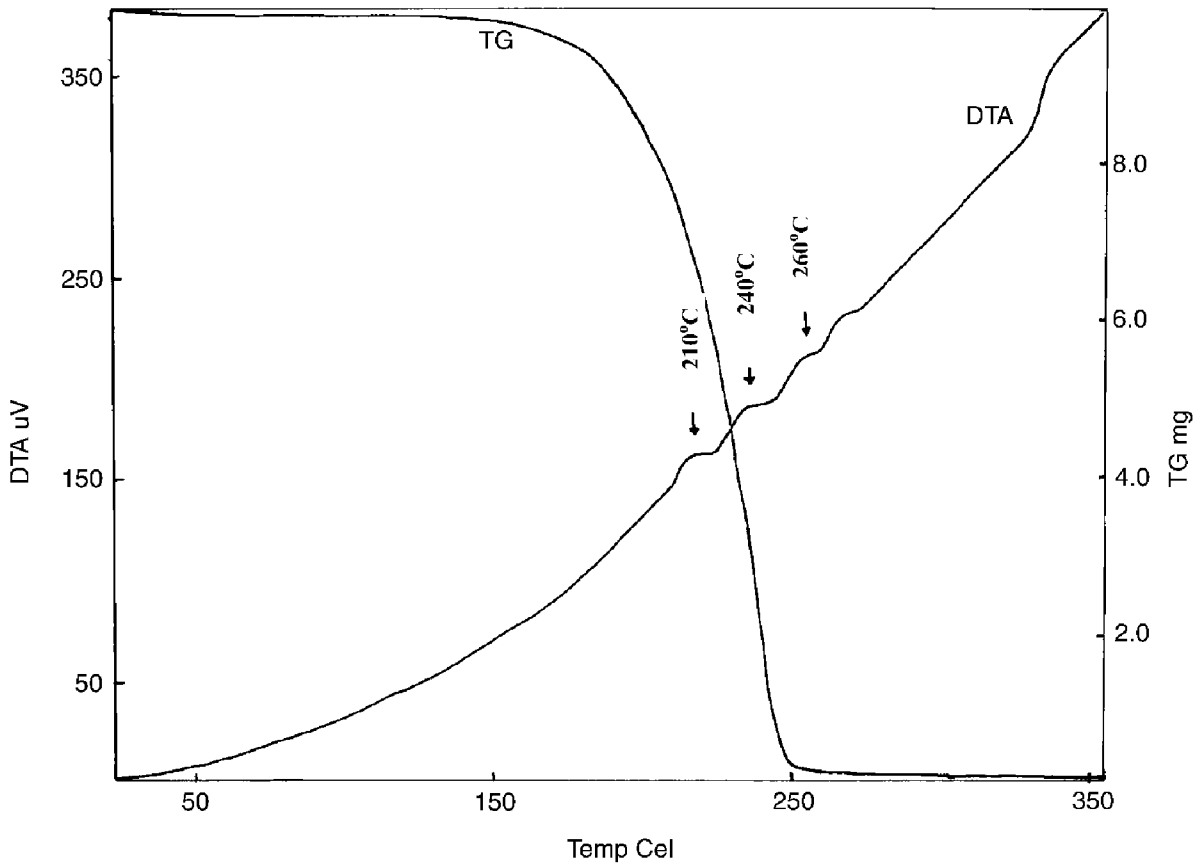

Figure 1. Simultaneous TG and DTA curves of un-irradiated $Ru(acac)_3$.

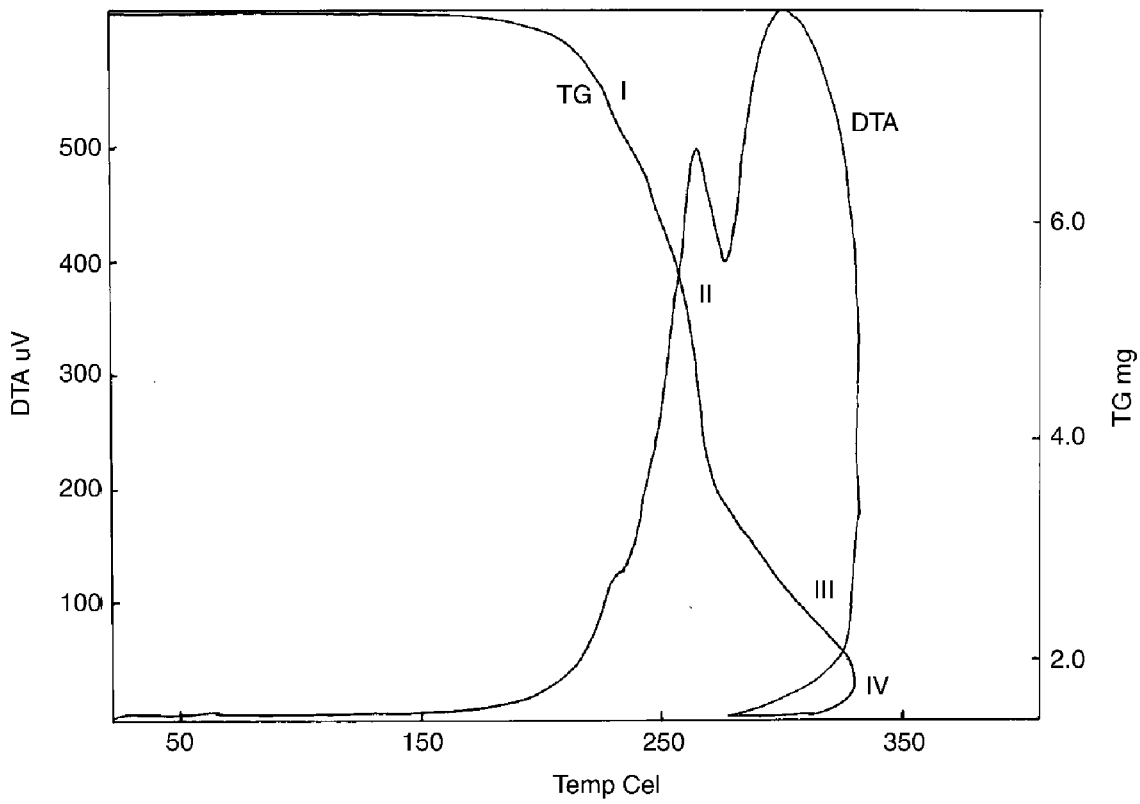

Figure 2. Simultaneous TG and DTA curves of γ-irradiated $Ru(acac)_3$.

The experimentally observed weight loss was found to exceed the predicted one as calculated according to Equation (10). This disagreement between the experimentally and theoretically calculated weight losses of the thermal decomposition of $Ru(acac)_3$ is most likely due to the sublimation of a small portion of $Ru(acac)_3$ in the thermal decomposition range of $Ru(acac)_3$. The DTA curve shows a superposition of several exothermic peaks in the temperature range from ≈210 °C to ≈280 °C, associated with the crystallization of RuO_2 and the decomposition of the acetylacetonate ligand. Figure 2 shows typical TG and DTA curves of γ-irradiated $Ru(acac)_3$ with 10^2 KGy total γ-ray dose. The TG showed a shift in the decomposition temperature range to higher values (200–320 °C) and the decomposition eventually goes to completion (*i.e.*, ≈100% weight loss). In the major decomposition step, it is possible to recognize four overlapping decomposition stages: I, II, III and IV. The decomposition stages I, II and III are associated with the decomposition of the acetylacetonate ligands, probably in three steps. The step IV decomposition exhibits a gain in the weight loss, attributed probably to the formation of a volatile Ru compound.

The dynamic data shown in Figures 3 and 4 were analysed using the Coats–Redfern method, Equation (5). Inserting various $g_j(\alpha)$ into these Equation results in a set of Arrhenius parameters

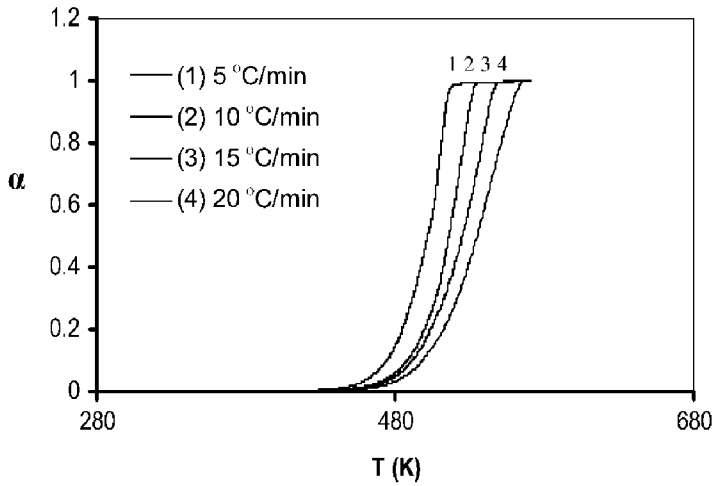

Figure 3. Thermogravimetric data showing the extent of un-irradiated $Ru(acac)_3$ conversion during non-isothermal decomposition. The heating rate of each experiment (in °C min^{-1}) is indicated by each curve.

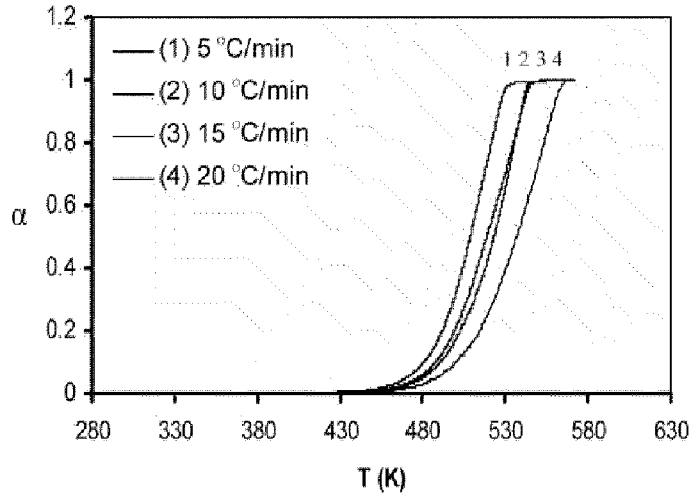

Figure 4. Thermogravimetric data showing the extent of γ-irradiated $Ru(acac)_3$ conversion during non-isothermal decomposition. The heating rate of each experiment (in °C min^{-1}) is indicated by each curve.

(E_a, ln A), as determined from the slopes and intercepts of the plots of the left sides of Equation (5) *vs.* $1/T_\alpha$. The Arrhenius parameters for the non-isothermal decomposition of un-irradiated and γ-irradiated $Ru(acac)_3$ with 10^2 KGy total γ-ray dose are listed in Table 2.

The results of applying the model-free iso-conversional method, Equations (7) and (8), to the non-isothermal decomposition data for both un-irradiated and γ-irradiated $Ru(acac)_3$ with total 10^2 KGy total γ-ray dose permits a determination of $E\alpha$ as a function of α, are shown in Figures 5 and 6.

5. Discussion

An examination of Table 2 shows that the Arrhenius parameters obtained for non-isothermal decomposition of $Ru(acac)_3$ are highly variable, exhibiting a strong dependency on the reaction model selected, with more than one reaction model showing that absolutely different mechanisms can correctly fit the experimental data. The reason for the failure of the application of the model-fitting method to the non-isothermal data is clear. Unlike in isothermal experiments, in which the temperature is isolated as an experimental variable, the non-isothermal experiments allow fits with simultaneously varying temperature sensitivity (E, ln A) and reaction model $f(\alpha)$. The basic assumption of the iso-conversional method is that the reaction model as defined in Equation (1) is not dependent on the temperature or heating rate. In contrast to model-fitting methods which provide a constant dependence of $E\alpha$ on α, the iso-conversional free methods show a dependence of $E\alpha$ on the extent of conversion as shown in Figures 5 and 6. The iso-conversional analysis for non-isothermal data showed a decrease in the value of $E\alpha$ with the extent of conversion α, with an average value centred at $\approx 112\ KJ\ mol^{-1}$, in good agreement with the values obtained using the model-fitting approach. The isoconversional curves obtained in this paper for non-isothermal decomposition of un-irradiated and γ-irradiated $Ru(acac)_3$ reveal a typical dependence for reversible reactions according to Vyazovkin et al. (*12*). Vyazovkin and Linert have shown that the decreasing dependence of $E\alpha$ on α corresponds to the kinetic scheme of an endothermic reversible reaction followed by an irreversible one. For such a process, E_a is limited by the sum of the activation energy of the irreversible reaction and the enthalpy of the reversible reaction at low conversions. At high values of conversion, α, E_a is limited by the activation energy of the irreversible reaction at high α (*13*).

The iso-conversional analysis using a modified Vyazovkin approach at different arbitrary heating programs $T_i(t)$ affords a different behaviour for the dependency of $E_{a,\alpha}$ on α (see Figure 6), and reflects the role of the heating rate in the non-isothermal decomposition of solids.

Table 2. Arrhenius parameters for non-isothermal decomposition of un-irradiated and γ-irradiated (10^2 KGy) $Ru(acac)_3$ at $10\ ^\circ C\ min^{-1}$ by Coats and Redfern.

	Un-irradiated		γ-irradiated (10^2 KGY)			
Model	E_a	ln A_j	r_j	E_a	ln A_j	R_j
R2	128.127	13.77168	0.9983	95.787	20.44391	0.9943
R3	136.723	15.50166	0.995	103.792	21.75681	0.9971
A2	155.962	19.82585	0.9822	119.0399	25.98113	0.9962
A3	155.962	18.51462	0.9822	119.0399	25.57513	0.9962
D1	220.5288	33.57618	0.9964	167.3691	36.96855	0.9765
D2	246.983	55.80501	0.9964	188.3869	41.5108	0.9893
D3	281.944	62.89396	0.9953	216.1557	46.87215	0.9974

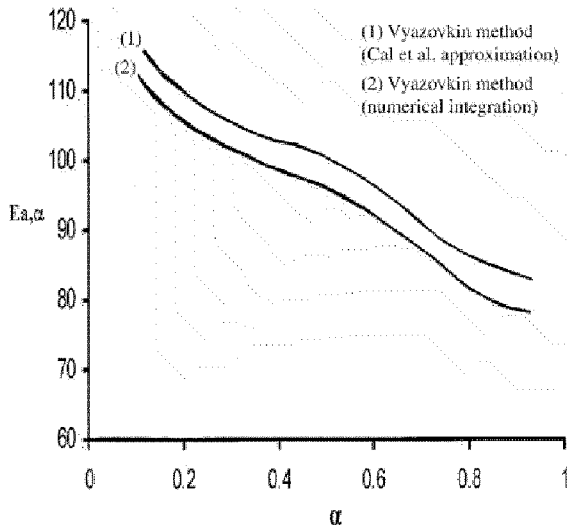

Figure 5. Dependence of the activation energy on the extent of conversion as determined by iso-conversional methods.

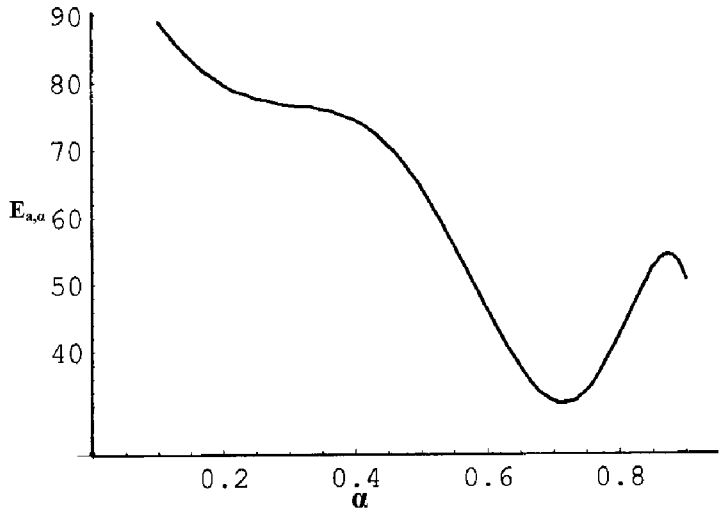

Figure 6. Dependencies of the activation energy on the extent of conversion as determined using a modified Vyazovkin iso-conversional method.

5.1. *IR and XRD measurements*

The physical and chemical changes induced by γ-irradiation in $Ru(acac)_3$ were followed by recording the IR spectra of the material before and after γ-irradiation. Figure 7 shows IR spectra of both un-irradiated and γ-irradiated $Ru(acac)_3$. Both spectra display the characteristic bands assigned to various vibration modes of acetylacetonate functional groups. Neither disappearance nor appearance of new bands was recorded in the IR spectrum of γ-irradiated $Ru(acac)_3$ with 10^2 total γ-ray dose, but a decrease was recorded in most characteristic bands. The band assigned to the ν Ru−O bond at 660 Cm^{-1} was more affected by irradiation than any other band in the spectrum. The decrease in intensity of this band could be attributed to bond scission and degradation caused by γ-irradiation. IR-bands for $Ru(acac)_3$ and their assignments are listed in Table 3.

It should be mentioned that the formation of the solid residue was initially started by formation of Ru metal. The Ru metal oxidizes into RuO_2 with the increase of the heating temperature as well as with prolonged heating at the same temperature. This prospect has been demonstrated by recording XRD patterns and IR spectra of the solid residue after calcinations of un-irradiated $Ru(acac)_3$ at different calcination temperatures for different time intervals. The sample calcined at 200 °C exhibits a non-crystalline behaviour, due to formation of Ru metal nanoparticles (*14*).

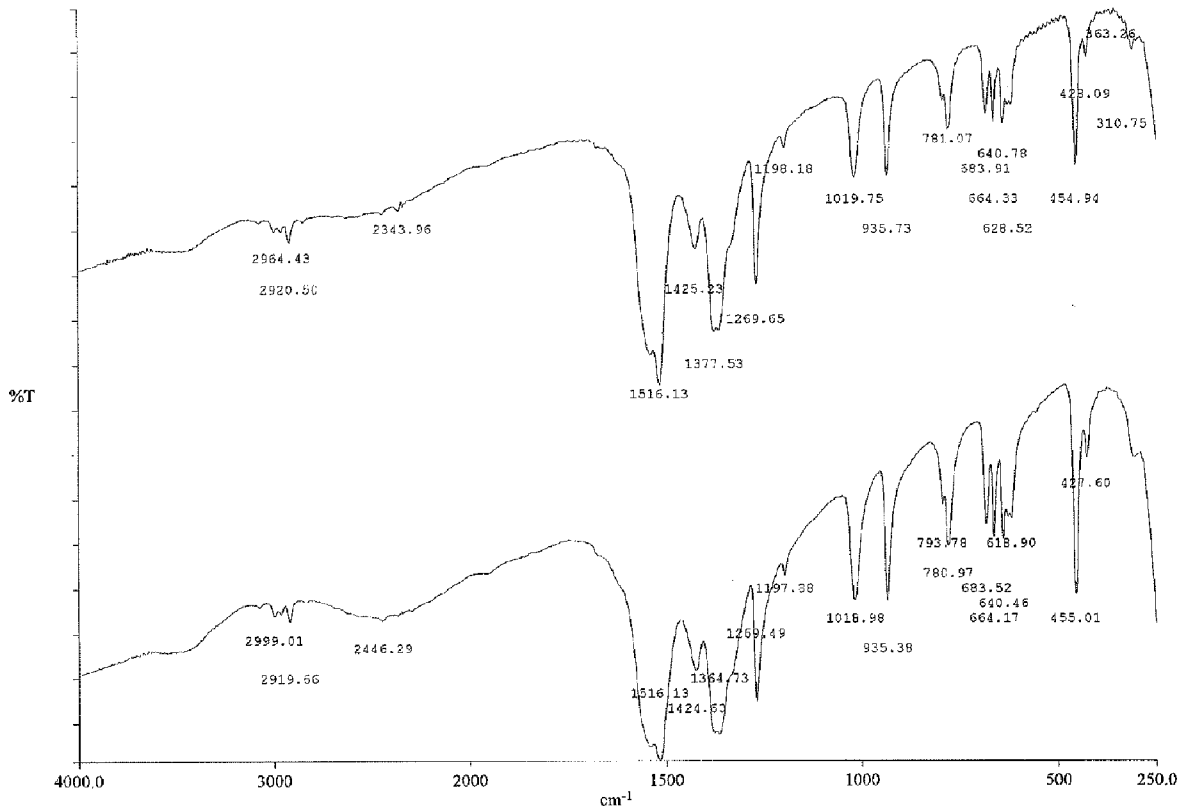

Figure 7. IR spectra of un-irradiated and γ-irradiated $Ru(acac)_3$.

Table 3. IR bands of $Ru(acac)_3$ and their assignments.

Band position		Assignment
$Ru(acac)_3$ γ-irradiated	$Ru(acac)_3$ un-irradiated	
2920.81	2929.66	ν(CH) $\nu(CH_3)$
1518.33	1518.33	$\nu(C{=}{=}C) + \nu(C{=}{=}C)$
1425.92	1424.60	δ_d (CH_3)
1377.81	1364.73	$\delta_s(CH_3)$
1269.75	1296.49	$\nu(C{-}CH_3) + \nu(C{=}{=}C)$
1019.91	1018.98	ρ_r (CH_3)
935.83	935.38	$\nu(C{=}C) + \nu(C{=}{=}O)$
781.41	780.97	π (CH)
688.38	683.52	ν(C-CH_3) + ring def.
664.19	660.17	ν RuO
		$\pi\left(CH_3{-}C\begin{matrix}C\\O\end{matrix}\right)$
640.68	640.46	
455.02	455.01	$\nu(C-CH_3) + \nu$RuO

The Bragg angle of $2\theta = 43.4°$ is consistent with the Ru(0) diffraction ($d = 0.208$ nm). The particle size calculated from the *Deby-Scherrer* formula using the information from this peak was ≈ 1.7 nm. The sample calcined at 300 °C exhibits crystalline peaks ascribed to Ru and RuO_2 crystallization (*15*). The XRD pattern of the sample heated at 600 °C showed diffraction lines attributed to the rutile-type RuO_2 as a single phase. The FT-IR spectrum for the sample heated at 600 °C exhibits a band at 967 cm^{-1} attributed to Ru=O, which is a metal-like conductor. The powder X-ray diffraction pattern of the γ-irradiated $Ru(acac)_3$ shows that new diffraction features are

not present in the XRD pattern of un-irradiated $Ru(acac)_3$. By heating the γ-irradiated $Ru(acac)_3$ sample with 10^2 and 10^3 KGy total γ-ray doses under the same experimental conditions as for the un-irradiated sample, one obtains a different set of XRD patterns. The result of these measurements will be published in a separate publication. Further studies concerning the formation of Ru and RuO_2 nanoparticles by thermal decomposition of un-irradiated and γ-irradiated $Ru(acac)_3$ are in progress in our laboratory.

6. Conclusions

The thermal decomposition behaviour of $Ru(acac)_3$ proceeds in one major decomposition step, with the formation of RuO_2 as solid residue. γ-irradiation up to a dose of 10^2 KGy appears to have no significant effect on the thermal behaviour of $Ru(accac)_3$. The Arrhenius parameters, the kinetic model and the dependence of E_a on α during the progress of the decomposition appear not to be largely affected by the γ-irradiation. The use of single-heating rate data for the determination of kinetic parameters should be avoided; free methods that use multi-heating rate data and assume a multi-step nature of the process can describe the course of a solid reaction sufficiently well. The single-heating rate technique and model-fitting mechanism are of limited help to deduce the correct and adequate kinetic parameters. The multi-step process using the multi-heating rate technique and model-free methods are rather typical for reactions of solids.

Acknowledgement

The main author (R.M. Mahfouz) is thankful to SABIC for financial support and the use of some measurement facilities.

References

(1) Vlaic, G.; Bart, J.C.J.; Cavigiolo W.; Furesi, A.; Ragani, V.; Sabadini, M.G.C.; Burattini, E. *J. Catal.* **1987,** *107,* 263–274.
(2) Coq, B.; Bittar, A.; Figueras, F. *Appl. Catal.* **1990,** *59,* 103–121.
(3) Coq, B.; Crabb, E.; Warawdekar, M.; Bond, G.C.; Slaa, J.C.; Galvagno, S.; Mercadante, L.; Ruitz, J.G.; Sierra, M.C.S. *J. Mol. Catal.* **1994,** *92,* 107–121.
(4) Lashdaf, M.; T. Hatanpää and Titta, M. *J. Therm. Anal. Calorim.* **2001,** *64,* 1171–1182.
(5) Bykov, A.F.; Morozova, N.B.; Igumenov, I.K.; Sysoev, S.V. *J. Therm. Anal. Calorim.* **1996,** *46,* 1551–1565.
(6) Music, S.; Popvic, S.; Maljkovic, M.; Gajovic, F.F. *J. Mat. Sci. Letters* **2002,** *21,* 1131–1134.
(7) Plyuto, V.Y.; Babich, V.I.; Sharanda, L.F.; Marco de Wit, A.; Mol, J.C. *Thermochim. Acta* **1999,** *335,* 87–91.
(8) Spinks, J.W.T.; Woods, J.R. *An Introduction to Radiation Chemistry*; Wiley: New York, 1990.
(9) Coats, W.A.; Redfern, P.J. *Nature* **1964,** *201,* 68–69.
(10) Vyazovkin, S.; Dollimore, D. *J. Chem. Inf. Comput. Sci.* **1996,** *36,* 42–45.
(11) Cai, J.; Yao, F.; Yi, W.; He, F. *AI ChE* **2006,** *52,* 1554–1557.
(12) Mahfouz, M.R.; Monshi, M.A.S.; Alshehri, S.M.; Abd El-Salam, N.M. *Rad. Phys. Chem.* **2000,** *59,* 381–385.
(13) Vyazovkin, S.; Linert, W. *J. Solid State Chem.* **1995,** *114,* 392–398.
(14) Salommonsson, A.; Petora, R.M. Jr.; Uvdal, K.; Aulin, C.; Käll, P.; Ojamäe, L.; Strand, M.; Sanati, M.; Spetz, A. *J. Nanoparticle Res.* **2006,** *8,* 899–910.
(15) Nakamoto, K. In *Infrared Spectra of Inorganic and Coordination Chemistry*; Wiley-Interscience: New York, 1970.